17

Self-Consistent Anharmonic Theory and Its Application to $BaTiO_3$ Crystal

Yutaka Aikawa
Taiyo Yuden Co, Ltd.
Japan

1. Introduction

Because phase transition is important in solid state physics, numerous attempts have thus far been made to study the nature of phase transitions in magnets, superconductors, ferroelectrics, and so on. For ferroelectrics, both phenomenological and microscopic approaches have been adopted to study phase transitions. Generally, it is considered that at high temperatures, the general phenomenological theory and first-principles calculations appears to be almost mutually exclusive.

It is well known that the phenomenological Landau theory of phase transitions can provide a qualitatively correct interpretation of the soft mode of ferroelectrics at the Curie temperature (L.D.Landau & E.M.Lifshitz, 1958); however, this theory cannot explain the mechanism of ferroelectric phase transition. Furthermore, the coefficients of the expansion terms of the Gibbs potential cannot be explained by the essential parameters derived by first-principles calculations. The first principles calculations were performed to determine the adiabatic potential surface of atoms, and the potential parameters were determined to recreate the original adiabatic potential surface. This procedure ensures a highly systematic study of ferroelectric properties without any reference to the experimental values.

In order to study the phase transition, Gillis et al. discussed first the instability phenomena in crystals, on the basis of a self-consistent Einstein model (N. S. Gills et al., 1968, 1971). In this model each atom is assumed to perform harmonic oscillation with the frequency which is self-consistently determined from the knowledge of interatomic potential in crystal and the averaged motions of all atoms. The effect of anharmonicity comes in through the self-consistent equations. T. Matsubara et al. applied this method to a simple one-dimensional model to discuss anharmonic lattice vibration, which is enhanced on and near the surface than in the interior (T. Matsubara & K. Kamiya,1977).

On the other hand, the combination of the results derived from first-principles calculations with the effective Hamiltonian method implemented by means of a Monte Carlo simulation (W. Zhong et al.,1995), seems to successfully explain the lattice strain change in $BaTiO_3$ at high temperatures. However, the abovementioned approach cannot explain the behavior of the dielectric property of materials at high temperatures during the phase transitions in the soft mode.

To discuss such high temperature transitions, K. Fujii et al. have proposed a self-consistent anharmonic model (K. Fujii et al., 2001), and the author has extended it to derive the ferroelectric properties of $BaTiO_3$ (Y.AIkawa et al., 2007, 2009), in other words, it has been shown that the ferroelectric properties of materials can be described by the interatomic potential, which is derived from first-principles calculations. In the present study we applied a theoretical method, namely, the self-consistent anharmonic theory, to study the cubic-to-tetragonal phase transition in practical applications. The author shows that the transition occurs in the soft mode, and that the relationship between the transition behavior in the high temperature region and the essential parameters at absolute zero temperature which can be derived using first-principles calculations.

In the previous study, the author introduces the anharmonicity not only into crystal potential but also into trial one in order to extend the self-consistent Einstein model, and succeeded to derive the soft mode frequency of $BaTiO_3$ crystal near the transition temperature, and showed that the softening phenomena never take place when harmonic oscillator is adopted as trial potential (Y. Aikawa & K. Fujii, 2010). Furthermore, it becomes possible to explain the relation between the dielectric property in high temperature and atomic potential at absolute zero temperature derived from first principles calculations (Y.Aikawa et al., 2009), and also to explain the isotope effect (Y.Aikawa et al., 2010a), surface effect (Y.Aikawa et al., 2010b; T. Hoshina et al., 2008), and so on.

2. Theoretical analysis

Landau constructed a phenomenological theory for the second order phase transition by considering only the symmetry change of a system (L. D. Landau & E. M. Lifshitz, 1958). Gibbs free energy is expanded by an order parameter σ in the vicinity of transition temperature as

$$G = G_0 + B(T_C - T)\sigma^2 + A\sigma^4 + \cdots$$

It is difficult to reflect microscopic information such as interactions between atoms in the expansion coefficients A, B and the transition temperature T_C.

K. Fujii et.al showed theoretically a softening mechanism from the variational principle at finite temperature (K. Fujii et al., 2001, 2003). In that work, the coefficients of the second and fourth order terms in a trial potential represented by an anharmonic oscillator system were expressed by the characteristic constants of interatomic potentials in a crystal. The author found that the temperature dependence of the coefficient of the second order term in the trial potential shows the same behavior as the Landau expansion. The softening phenomena are discussed on the basis of the temperature- and wave vector-dependence of the expansion coefficient near the instability temperature, and the soft mode is identified by introducing normal coordinates instead of direct atomic displacements.

It is considered a crystal system consisting of N atoms. Let $\boldsymbol{x}_n$ be coordinate of the n-th atom whose mass is m_n. The Hamiltonian of this system is given by

$$H = \frac{1}{2}\sum_n m_n \dot{\boldsymbol{x}}_n^2 + \sum_{nn'} V\left(\left|\boldsymbol{x}_n - \boldsymbol{x}_{n'}\right|\right) \quad , \tag{1}$$

where V are interatomic pair potentials. An interatomic distance between atoms n and n' is given by

$$\boldsymbol{X}_n - \boldsymbol{X}_{n'} = \boldsymbol{a}_{nn'} + \boldsymbol{u}_n - \boldsymbol{u}_{n'} \quad , \tag{2}$$

where $\boldsymbol{a}_{nn'}$ means the interatomic distance in equilibrium state and $\boldsymbol{u}_n$ denotes an atomic displacement from the equilibrium position. The displacement $u_{n,\alpha}$ in the α direction is expanded by using the eigenfunctions $e_{n,\alpha}^{(S)}$ of a dynamical matrix as

$$u_{n,\alpha} = \sum_S m_n^{-1/2} e_{n,\alpha}^{(S)} Q_S \qquad (S = 1, 2, \cdots, 3N) \quad , \tag{3}$$

where Q_S are the normal coordinates. The interatomic distance is represented by

$$\left|\boldsymbol{X}_n - \boldsymbol{X}_{n'}\right| = \left|\boldsymbol{a}_{nn'}\right| + \sum_S c_S^{(nn')} Q_S \quad , \tag{4}$$

where $c_S^{(nn')}$ are defined by using the the direction cosine, $\ell_{nn',\alpha}$, of the interatomic distance vector as (α=x,y,z)

$$c_S^{(nn')} = \sum_\alpha \ell_{nn',\alpha} \left(m_n^{-1/2} e_S^{(n\alpha)} - m_{n'}^{-1/2} e_S^{(n'\alpha)} \right) \quad . \tag{5}$$

Then, Hamiltonian is rewritten in terms of the normal coordinates Q_S as (Y. Aikawa & K. Fujii, 1993)

$$H = \frac{1}{2} \sum_S \dot{Q}_S^2 + \sum_{n,n'} V\left(\left|\boldsymbol{a}_{nn'}\right| + \sum_S c_S^{(nn')} Q_S \right) \quad , \tag{6}$$

The variational principle at finite temperature is applied to obtain thermal properties of the crystal. In this method, an anharmonic oscillator with the fourth order term is adopted as a trial Hamiltonian H_{tr}, (Y. Aikawa & K. Fujii, 2009)

$$H_{tr} = \frac{1}{2} \sum_S \dot{Q}_S^2 + \sum_S A_S Q_S^4 + \sum_S B_S Q_S^2 \quad . \tag{7}$$

The thermal average of a physical quantity $X\left(\dot{Q}_S, Q_S\right)$ is given by

$$\begin{aligned} \left\langle X\left(\dot{Q}_S, Q_S\right) \right\rangle &= \mathrm{Tr}\left[\rho X\left(\dot{Q}_S, Q_S\right) \right] \\ &= \frac{\int_{-\infty}^{\infty} X\left(\dot{Q}_S, Q_S\right) \exp\left(-H_{tr}/\mathrm{k_B}T\right) \prod_S \mathrm{d}\dot{Q}_S \mathrm{d}Q_S}{\int_{-\infty}^{\infty} \exp\left(-H_{tr}/\mathrm{k_B}T\right) \prod_S \mathrm{d}\dot{Q}_S \mathrm{d}Q_S} \end{aligned} \tag{8}$$

The free energy of the crystal is given by

$$\begin{aligned} F &= \left\langle H \right\rangle - \left\langle H_{tr} \right\rangle + F_{tr} \\ &= \left\langle \sum_{n,n'} V\left(\left|\boldsymbol{a}_{nn'}\right| + \sum_S c_S^{(nn')} Q_S \right) \right\rangle - \sum_S A_S \left\langle Q_S^4 \right\rangle - \sum_S B_S \left\langle Q_S^2 \right\rangle + F_{tr} \quad . \end{aligned} \tag{9}$$

The free energy F_{tr} of the trial system is also calculated by using the relation $F_{tr} = -\mathrm{k_B}T \ln Z_{tr}$. The partition function Z_{tr} is represented by using the variables $y_S^4 \equiv A_S Q_S^4 / \mathrm{k_B}T$ and $p_S \equiv \sqrt{1/4A_S \, \mathrm{k_B}T} \; B_S$ as:

$$
\begin{aligned}
Z_{tr} &= \frac{1}{\mathrm{h}^{6N}} \int_{-\infty}^{\infty} \exp\left(-H_{tr}/\mathrm{k_B}T\right) \prod_S \mathrm{d}\dot{Q}_S \mathrm{d}Q_S \\
&= \frac{1}{\mathrm{h}^{6N}} \left(\sqrt{2\pi \mathrm{k_B}T}\right)^{3N} \prod_S \sqrt[4]{\frac{\mathrm{k_B}T}{A_S}} \int_{-\infty}^{\infty} \exp\left(-y_S^2 - 2p_S y_S^2\right) \mathrm{d}y_S \\
&\equiv \frac{1}{\mathrm{h}^{6N}} \left(\sqrt{2\pi \mathrm{k_B}T}\right)^{3N} \prod_S \sqrt[4]{\frac{\mathrm{k_B}T}{A_S}} z(p_S) \quad ,
\end{aligned}
\tag{10}
$$

where $z(p_S)$ satisfies a differential equation (Y. Onodera,1970):

$$
\frac{\mathrm{d}^2 z(p_S)}{\mathrm{d}p_S^2} - 2p_S \frac{\mathrm{d}z(p_S)}{\mathrm{d}p_S} - z(p_S) = 0 \quad . \tag{11}
$$

The solution $z(p_S)$ is expressed later by the confluent hyper geometric function. The thermal averages of y_S^2 and y_S^4 are easily obtained as

$$
\begin{aligned}
\left\langle y_S^2 \right\rangle &= -\frac{1}{2} \frac{\mathrm{d}}{\mathrm{d}p} \ln z(p_S) \\
\left\langle y_S^4 \right\rangle &= -p \left\langle y_S^2 \right\rangle + \frac{1}{4} \quad .
\end{aligned}
\tag{12}
$$

Thus,

$$
\left\langle Q_S^4 \right\rangle = -\frac{B_S}{2A_S} \left\langle Q_S^2 \right\rangle + \frac{1}{4\beta A_S} \quad . \tag{13}
$$

The free energy given by eq. (9) is rewritten as

$$
\begin{aligned}
F = &\sum_{nn'} \sum_S \int \mathrm{d}q V_q \exp\left[\mathrm{i}q \left| \boldsymbol{a}_{nn'} \right| + \sum_{\ell=1}^{\infty} \frac{(\mathrm{i}q)^\ell}{\ell!} \left(\sum_S 1 \right)^{\ell/2-1} c_S^{(nn')\ell} \left\langle Q_S^\ell \right\rangle_C \right] \\
&- \frac{1}{2} \sum_S B_S \left\langle Q_S^2 \right\rangle - \mathrm{k_B}T \sum_S \ln \frac{\mathrm{e}^{1/4} \left(\mathrm{k_B}T\right)^{3/4} z(P_S)}{(2\pi)^{3/2} \hbar^2 A_S^{1/4}} \quad .
\end{aligned}
\tag{14}
$$

where the potential is decomposed into the Fourier component. The notation $\langle \cdots \rangle_C$ denotes the cumulant as defined by

$$
\sum_{\ell=0}^{\infty} \frac{\phi^\ell}{\ell!} \left\langle x^\ell \right\rangle = \exp\left(\sum_{\ell=1}^{\infty} \frac{\phi^\ell}{\ell!} \left\langle x^\ell \right\rangle_{\mathrm{C}} \right) \quad , \tag{15}
$$

It is evident from the formula of the trial Hamiltonian that

$$
\left\langle Q_S^n \right\rangle_0 = \begin{cases} 0 & n : odd \\ \left\langle Q_S^n \right\rangle_0 & n : even \end{cases} \quad ,
$$

thus the cumulant expansions are as follows:

$$\begin{aligned}\left\langle Q_S^2\right\rangle_C &= \left\langle Q_S^2\right\rangle \\ \left\langle Q_S^4\right\rangle_C &= \left\langle Q_S^4\right\rangle_0 - 3\left\langle Q_S^2\right\rangle^2 \\ &= -\frac{B_S}{2A_S}\left\langle Q_S^2\right\rangle + \frac{\mathrm{k_B}T}{4A_S} - 3\left\langle Q_S^2\right\rangle^2 \\ &\cdots\end{aligned} \tag{16}$$

From the variation of the free energy with the interatomic distance $|\boldsymbol{a}_{nn'}|$, we have the equation

$$\frac{\partial\langle V\rangle}{\partial|\boldsymbol{a}_{nn'}|} = 0 \quad . \tag{17}$$

From the optimum condition $\partial F/\partial A_S = 0$ gives the relation

$$\begin{aligned}&\sum_{nn'}\int \mathrm{d}qV_q \exp\left[\mathrm{i}q|\boldsymbol{a}_{nn'}| + \sum_{\ell=1}^{\infty}\frac{(\mathrm{i}q)^\ell}{\ell!}\left(\sum_S 1\right)^{\ell/2-1} c_S^{(nn')\ell}\left\langle Q_S^\ell\right\rangle_{\mathrm{C}}\right]\sum_{\ell=1}^{\infty}\frac{(\mathrm{i}q)^\ell}{\ell!}\left(\sum_{\mathrm{S}} 1\right)^{\ell/2-1} c_S^{(nn')\ell}\frac{\partial\left\langle Q_S^\ell\right\rangle_{\mathrm{C}}}{\partial A_S} \\ &-\frac{1}{2}B_S\frac{\partial\left\langle Q_S^\ell\right\rangle_0}{\partial A_S} - \frac{B_S}{2A_S}\left\langle Q_S^\ell\right\rangle_0 + \frac{\mathrm{k_B}T}{4A_S} = 0 \quad .\end{aligned} \tag{18}$$

The optimum condition $\partial F/\partial B_S = 0$ gives the relation

$$\begin{aligned}&\sum_{nn'}\int \mathrm{d}qV_q \exp\left[\mathrm{i}q|\boldsymbol{a}_{nn'}| + \sum_{\ell=1}^{\infty}\frac{(\mathrm{i}q)^\ell}{\ell!}\left(\sum_S 1\right)^{\ell/2-1} c_S^{(nn')\ell}\left\langle Q_S^\ell\right\rangle_{\mathrm{C}}\right]\sum_{\ell=1}^{\infty}\frac{(\mathrm{i}q)^\ell}{\ell!}\left(\sum_{S} 1\right)^{\ell/2-1} c_S^{(nn')\ell}\frac{\partial\left\langle Q_S^\ell\right\rangle_{\mathrm{C}}}{\partial B_S} \\ &-\frac{1}{2}B_S\frac{\partial\left\langle Q_S^\ell\right\rangle_0}{\partial B_S} + \frac{1}{2}\left\langle Q_S^\ell\right\rangle_0 = 0 \quad .\end{aligned} \tag{19}$$

From eq. (18) and eq. (19), an equation to be satisfied in the thermal equilibrium state is obtained as

$$\left[\frac{B_S}{A_S} - \frac{1}{2A_S}\sum_{nn'} c_S^{(nn')2}\frac{\partial^2\langle V_S\rangle}{\partial|\boldsymbol{a}_{nn'}|^2} + 6\left\langle Q_S^2\right\rangle_0\right]\left[\left\langle Q_S^2\right\rangle_0\frac{\partial\left\langle Q_S^2\right\rangle_0}{\partial A_S} + \frac{1}{A_S}\left(B_S\left\langle Q_S^2\right\rangle_0 - \frac{1}{2}\mathrm{k_B}T\right)\frac{\partial\left\langle Q_S^2\right\rangle_0}{\partial B_S}\right] = 0 . \tag{20}$$

It is obtained the solution for the anharmonic system as follows:

$$\frac{B_S}{A_S} - \frac{1}{2A_S}\sum_{nn'} c_S^{(nn')2}\frac{\partial^2\langle V_S\rangle}{\partial|\boldsymbol{a}_{nn'}|^2} + 6\left\langle Q_S^2\right\rangle_0 = 0 \quad . \tag{21}$$

Substituting eq. (21) into eq. (19), an important equation to determine the equilibrium condition for the free energy is obtained as

$$1 - \frac{1}{24A_S}\sum_{nn'} c_S^{(nn')4}\sum_S 1\ \frac{\partial^4\langle V_S\rangle}{\partial|\boldsymbol{a}_{nn'}|^4} = 0 . \tag{22}$$

In high temperature region ($p \ll 1$), the solution for eq. (11) is given by

$$\begin{aligned} z(p) &= \tfrac{1}{2}\Gamma\left(\tfrac{1}{4}\right) \mathrm{F}\left(\tfrac{1}{4}, \tfrac{1}{2}; p^2\right) - \Gamma\left(\tfrac{3}{4}\right) p \mathrm{F}\left(\tfrac{3}{4}, \tfrac{3}{2}; p^2\right) \\ &= \tfrac{1}{2}\Gamma\left(\tfrac{1}{4}\right)\left[1 - 2\delta p + \tfrac{1}{2} p^2 - \delta p^3 + \tfrac{5}{24} p^4 - \tfrac{7}{20} p^5 + \cdots\right] \quad , \end{aligned} \tag{23}$$

where $\delta \equiv \Gamma\left(\tfrac{3}{4}\right) / \Gamma\left(\tfrac{1}{4}\right) \cong 0.338$ and F is the confluent hyper geometric function defined as

$$\mathrm{F}(\alpha, \gamma; z) = 1 + \frac{\alpha}{\gamma} \frac{z}{1!} + \frac{\alpha(\alpha+1)}{\gamma(\gamma+1)} \frac{z^2}{2!} + \cdots \quad , \tag{24}$$

As a result, the average of $Q_S{}^2$ is determined as

$$\left\langle Q_S^2 \right\rangle = \sqrt{\frac{\mathrm{k_B} T}{A_S}} \left[\delta - \tfrac{1}{2}\left(1 - 4\delta^2\right) p_S + 4\delta^3 p_S^2 + \cdots \right] \tag{25}$$

In high temperature approximation, the equation for A_S to satisfy eqs. (21) and (25) is obtained as

$$A_S \cong \frac{\mathrm{k_B} T}{4 f^2} \left(\delta^2 + \frac{2\mathrm{C} f}{\nu_S} \right) \quad , \tag{26}$$

where C = $\delta^2 - 1/2$ and

$$\nu_S \equiv \frac{\mathrm{k_B} T}{2 B_S} \quad , \tag{27}$$

$$f \equiv \frac{\sum_{nn'} c_S^{(nn')2} \dfrac{\partial^2 \langle V_S \rangle}{\partial \left| \boldsymbol{a}_{nn'} \right|^2}}{\sum_{nn'} c_S^{(nn')4} \dfrac{\partial^4 \langle V_S \rangle}{\partial \left| \boldsymbol{a}_{nn'} \right|^4} \sum_S 1} \quad . \tag{28}$$

To substitute eq. (26) into eq.(22), the equation for determining the instability phenomena in the crystal is obtained as

$$\frac{\mathrm{k_B} T}{f^{(2)}} = \frac{f}{6\left(\delta^2 + \dfrac{2\mathrm{C} f}{\nu_S} \right)} \quad , \tag{29}$$

where

$$f^{(2)} \equiv \sum_{nn'} c_S^{(nn')2} \frac{\partial^2 \langle V_S \rangle}{\partial \left| \boldsymbol{a}_{nn'} \right|^2} \quad . \tag{30}$$

3. Soft mode

The aim of this section is as follows: the author derives equations to determine the soft mode which minimizes the ***k***-dependent part of the second order term in the trial potential,

and apply the result to the transition from cubic to tetragonal phase in a ferroelectric crystal $BaTiO_3$. The force constants between atoms are estimated by comparing the theoretical result for dispersion relations derived from a dynamical matrix with that of a neutron diffraction experiment (G. Shirane et.al., 1967; B. Jannet et al., 1984). The author applies the result to determination equations, and verify that the lowest frequency mode at Γ point corresponds to a mode causing the ferroelectric phase transition of $BaTiO_3$.

3.1 Determination equations for the soft mode

It is considered that the crystal instability takes place when the coefficient of the second order term in the trial potential becomes infinitesimal as temperature approaches to the transition point. Namely, the parameter ν_S increases to an unlimited extent. This type of phase transition accompanied by the symmetry change is suggested as the softening in the crystals (W. Cochran, 1959). The instability temperature T_C is defined by the temperature where $\nu_S \to \infty$ in eq.(29) as

$$\frac{k_B T_C}{f_\infty^{(2)}} = \frac{f_\infty}{6\delta^2} \quad . \tag{31}$$

where f_∞ and $f_\infty^{(2)}$ mean the values of f and $f^{(2)}$ under $\nu_S \to \infty$. In the vicinity of the instability temperature, the parameter ν_S can be represented from eqs.(29) and (31) as:

$$\frac{1}{\nu_S} \cong \frac{3\delta^4}{C f_\infty^2 f_\infty^{(2)}} k_B (T_C - T) \quad , \tag{32}$$

where the instability temperature is obtained as

$$T_C = \frac{k_B}{6\delta^2} \frac{\left(\sum_{nn'} c_S^{(nn')2} \left. \frac{\partial^2 \langle V_S \rangle}{\partial |\boldsymbol{a}_{nn'}|^2} \right|_{\nu_S \to \infty} \right)^2}{\sum_{nn'} c_S^{(nn')4} \sum_S 1 \left. \frac{\partial^4 \langle V_S \rangle}{\partial |\boldsymbol{a}_{nn'}|^4} \right|_{\nu_S \to \infty}} \quad . \tag{33}$$

Consequently, the variational parameter of the second order term is given as

$$B_S = \frac{\delta^2}{4C} \frac{\sum_{nn'} c_S^{(nn')4} \sum_S 1 \left. \frac{\partial^4 \langle V_S \rangle}{\partial |\boldsymbol{a}_{nn'}|^4} \right|_{\nu_S \to \infty}}{\sum_{nn'} c_S^{(nn')2} \left. \frac{\partial^2 \langle V_S \rangle}{\partial |\boldsymbol{a}_{nn'}|^2} \right|_{\nu_S \to \infty}} k_B (T_C - T) \quad , \tag{34}$$

and the variational parameter of the forth order term is also calculated as:

$$A_S = \frac{1}{24} \sum_{nn'} c_S^{(nn')4} \sum_S 1 \left. \frac{\partial^4 \langle V_S \rangle}{\partial |\boldsymbol{a}_{nn'}|^4} \right|_{\nu_S \to \infty} \quad . \tag{35}$$

Near the instability temperature, the optimum value of the trial potential is represented as

$$\left\langle V_{R,\boldsymbol{k}} \right\rangle = B_R(\boldsymbol{k})(T_{\mathrm{C}} - T)\left\langle Q_{R,\boldsymbol{k}}^2 \right\rangle + A_{R,\boldsymbol{k}} \left\langle Q_{R,\boldsymbol{k}}^4 \right\rangle \quad , \tag{36}$$

where the degree of freedom of the system, $S = 3N$, is replaced by the branch and the wave vector $(R, \boldsymbol{k})$. In order that the softening may actually occur, it is necessary that $B_R(\boldsymbol{k})$ becomes minimum at the definite $\boldsymbol{k}$ vector which is written as

$$B_R(\boldsymbol{k}) = \frac{\delta^2 \mathrm{k_B}}{4\mathrm{C}} \frac{\sum_{nn'} c_{R,\boldsymbol{k}}^{(nn')4} \sum_{R,\boldsymbol{k}} 1 \dfrac{\partial^4 \langle V \rangle}{\partial |\boldsymbol{a}_{nn'}|^4}\Big|_{V_{\boldsymbol{k}} \to \infty}}{\sum_{nn'} c_{R,\boldsymbol{k}}^{(nn')2} \dfrac{\partial^2 \langle V \rangle}{\partial |\boldsymbol{a}_{nn'}|^2}\Big|_{V_{\boldsymbol{k}} \to \infty}} \propto \gamma_R(\boldsymbol{k}) \quad , \tag{37}$$

where $\gamma_R(\boldsymbol{k})$ is the $\boldsymbol{k}$-dependent part in $B_R(\boldsymbol{k})$ as

$$\gamma_R(\boldsymbol{k}) \equiv \frac{\sum_{nn'} c_{R,\boldsymbol{k}}^{(nn')4} \sum_{R,\boldsymbol{k}} 1}{\sum_{nn'} c_{R,\boldsymbol{k}}^{(nn')2}} \quad , \tag{38}$$

$$c_{R,\boldsymbol{k}}^{(nn')} = \sum_{\alpha} \ell_{nn',\alpha} \left(m_n^{-1/2} e_{R,\boldsymbol{k}}^{(n,\alpha)} - m_{n'}^{-1/2} e_{R,\boldsymbol{k}}^{(n'\alpha)} \right) \quad . \tag{39}$$

Here, the eigenfunctions $e_{R,\boldsymbol{k}}^{(n,\alpha)}$ of the dynamical matrix given approximately in Appendix can be easily derived. Consequently, determination equations for the soft mode identified by $(R, \boldsymbol{k})$ are given by

$$\mathrm{grad}\,\gamma_R(\boldsymbol{k}) = 0, \qquad \nabla^2 \gamma_R(\boldsymbol{k}) > 0 \quad . \tag{40}$$

First, whether or not the crystal instability takes place is decided by the temperature dependence of the second order term in the trial potential as shown in eq. (36). Next, the soft mode is identified by the determination equations formalized by eq.(40). To apply the equations, the eigenfunctions included in eq. (39) are necessary which are obtained through the eigenvalue problem of the dynamical matrix. Landau theory presents that only one irreducible representation takes part in the phase transition accompanied by the symmetry change. When more than two modes belong to the same irreducible representation, it is unknown which mode corresponds to the soft mode with the lowest frequency. In this section, the author shows that one can solve this difficulty by using eq.(40) as the determination equations for the soft mode.

3.2 Application to the ferroelectric crystal $BaTiO_3$

The author constructs a formalism to specify the atomic displacement pattern in softening of the $BaTiO_3$ crystal. The Bravais lattice of this crystal above the transition temperature is a cubic lattice whose unit cell and Brillouin zone are shown in Fig.1.

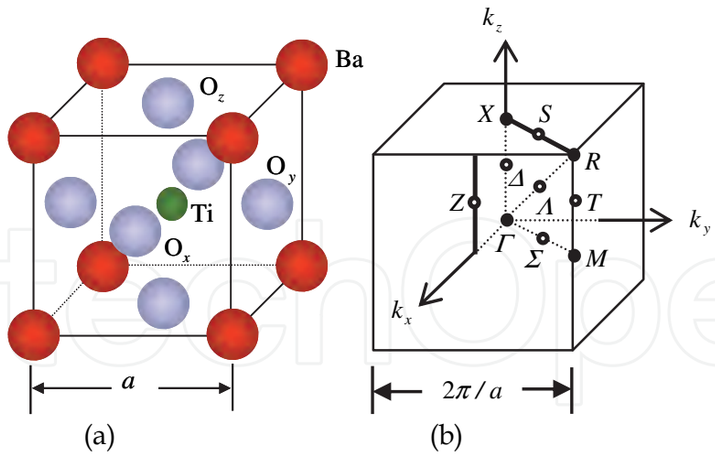

Fig. 1. Cubic structure and Brillouin zone of $BaTiO_3$ at high temperature. (a)The atoms in a unit cell are arranged at the original (n_x, n_y, n_z) for Ti, the corner (n_x+1/2, n_y+1/2, n_z+1/2) for Ba and the face center (n_x+1/2, n_y, n_z) for O, respectively. The atomic masses are defined as M_B, M_T and M_O for Ba, Ti and O, respectively. (b) The optical modes discussed in this work are restricted within the neighborhood of Γ point along the k_Z axis limits.

When the temperature decreases just below the transition temperature, a freezing of the mode that Ti and O ions vibrate reversely along the <001> direction of the crystal causes the structural phase transition from cubic to tetragonal symmetry under softening.

The atomic displacement patterns for vibrational modes at Γ point belonging to the irreducible representation of space group O_h^1 are derived by using the method of projection operator as (G. Burns, 1977)

$$4T_{1u} + T_{2u} \quad , \tag{41}$$

These modes are three-fold degenerate in accordance with the three-dimensional irreducible representation T. There are five branches which consist of one acoustical branch and four optical branches, named A, O_1, O_2, O_3 and O_4. The Slater(*S*), Last (*L*), Bending (*B*) modes and so on can be constructed by a combination of atomic displacements which form the basis functions of T_{1u}. However, one is not able to decide from the group theory which mode appears actually.

The dispersion relations $\omega^2_{R,\boldsymbol{k}}$ depend upon the force constants, shown in Fig. 2 , which are derived from the second-order derivative of the interatomic potential with respect to the interatomic distance, and defined as

$$\alpha = \kappa_{\mathrm{Ti-O}}, \quad \beta = \kappa_{\mathrm{Ba-O}}, \quad \eta = \kappa_{\mathrm{O-O}}, \quad \gamma = \kappa_{\mathrm{Ba-Ti}} \quad , \tag{42}$$

where

$$\kappa_{nn'} = \left. \frac{\partial^2 \left\langle V\left(\left|\boldsymbol{a}_{nn'}\right| + \sum_S c_S^{(nn')} Q_S \right) \right\rangle}{\partial \left(\left|\boldsymbol{a}_{nn'}\right| + \sum_S c_S^{(nn')} Q_S \right)^2} \right|_{\left|\boldsymbol{a}_{nn'}\right|} .$$

It is, however, difficult to estimate the force constants because the various interactions between atoms exist. The author attempt to decide them so as not to contradict the results by the neutron diffraction experiment (G.Shirane et al., 1967; B. Jannet et al.,1984).

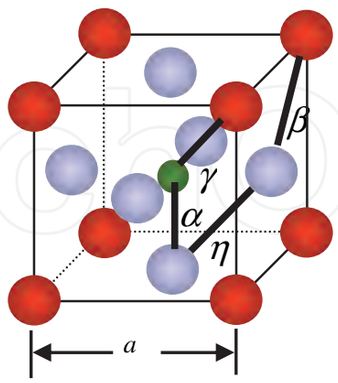

Fig. 2. Definition of the force constants between atoms: α, β, γ and η for Ti-O, Ba-O, Ti-Ba and O-O, respectively.

All the six optical modes which are capable of appearing under the various force constants are obtained by solving the dynamical matrix. In the low frequency region of the dispersion

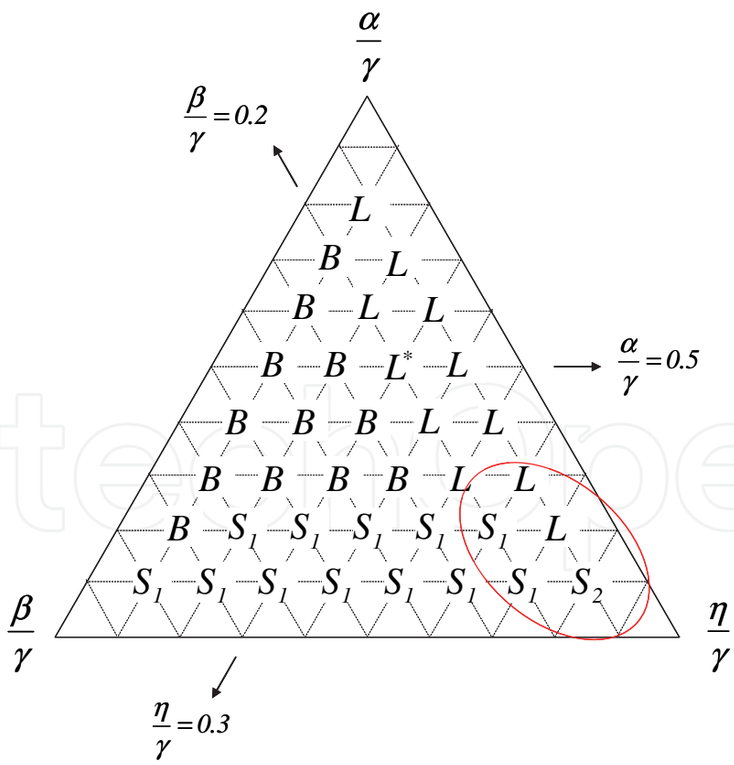

Fig. 3. Triangular diagram composed of the relative force constants $(\alpha/\gamma,\ \beta/\gamma,\ \eta/\gamma)$. The notation L* means that the Last mode corresponds to the lowest frequency mode at the coordinates $(\alpha/\gamma = 0.5,\ \beta/\gamma = 0.2,\ \eta/\gamma = 0.3)$.

curves, only two modes always appear within the set of four modes L, B, S_1 and S_2. The other two modes T_{2u} and *Plane* appear constantly in the high frequency region. It is well-known that the Slater mode is considered to be an optical lattice vibration in which Ti-sublattice vibrates in the reverse direction to O-octahedron. Until now, it has been sufficient to treat the displacements for only Ti and O ions, to explain qualitatively the appearance of an electric polarization. Though the motion of Ba-sublattice has been neglected in the past, the displacements for Ba ions must be considered in the case that the dispersion relations are compared between the theory proposed here and the experiment by the neutron diffraction. There are two kinds of the Slater mode: S_1 in which Ti-sublattice vibrates in the reverse direction to Ba-sublattice and O-octahedrons, and S_2 in which Ba-sublattice and Ti-sublattice vibrate in the reverse direction to O-octahedrons.

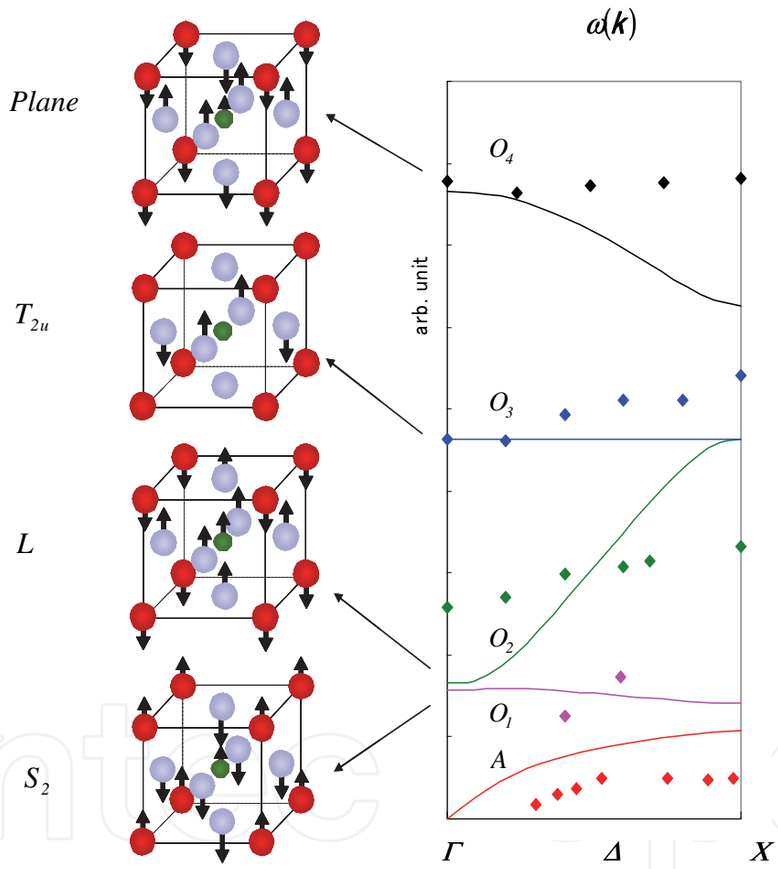

(a) (b)

Fig. 4. Dispersion curves with the force constants (α/γ =0.1, β/γ =0.09, η/γ =0.81) of $BaTiO_3$. (a) The lowest frequency mode at Γ point for each branch is shown with the atomic displacement patten. (b) The solid curves represent the theoretical values for the dispersion relations derived from eq. A-1. Small rectangles correspond to the experimental results. (Y.Aikawa & K.Fujii, 2011 to be published in Ferrolelectrics)

The triangular coordinates are introduced whose three axes mean the ratio of α, β and η normalized by γ, namely, α/γ, β/γ, η/γ. The triangular diagram in Fig.3 shows

which mode corresponds to the lowest frequency mode for the given coordinates at Γ point in the Brilloin zone. The dispersion relations within the region enclosed with an ellipse are in agreement with the results obtained by the neutron diffraction experiment. The lowest frequency mode is S_2 mode at the coordinates (α/γ =0.1, β/γ =0.09, η/γ =0.81) in the enclosed region.

The dispersion curves with the force constants $(\alpha/\gamma=0.1,\beta/\gamma=0.09,\eta/\gamma=0.81)$ of $BaTiO_3$ and the experimental values obtained by the neutron diffraction are shown in Fig. 4. Conversely, the author can estimate the relative force constants of the $BaTiO_3$ crystal by the above coordinates.

The (R, $\boldsymbol{k}$)-dependent part, $\gamma_R(\boldsymbol{k})$, for the coefficient $B_R(\boldsymbol{k})(T_C-T)$ of the second order term in the trial potential is given by

$$\gamma_R(\boldsymbol{k})=\frac{\left(c_{R,\boldsymbol{k}}^{(\mathrm{Ti-O})4}+c_{R,\boldsymbol{k}}^{(\mathrm{Ba-O})4}+c_{R,\boldsymbol{k}}^{(\mathrm{O-O})4}+c_{R,\boldsymbol{k}}^{(\mathrm{Ti-Ba})4}\right)\sum_{\boldsymbol{k}}1}{c_{R,\boldsymbol{k}}^{(\mathrm{Ti-O})2}+c_{R,\boldsymbol{k}}^{(\mathrm{Ba-O})2}+c_{R,\boldsymbol{k}}^{(\mathrm{O-O})2}+c_{R,\boldsymbol{k}}^{(\mathrm{Ti-Ba})2}}\quad , \tag{43}$$

It is to be noted that the functions $c_{R,\boldsymbol{k}}^{(nn')}$ are given by the eigenfunctions of the dynamical matrix which is dependent on the force constants. The author has found that the O_1 branch corresponding to the S_2 mode at Γ point tends to decrease in approaching to Γ point and satisfies with the condition given by eq.(40) as shown in Fig. 5.

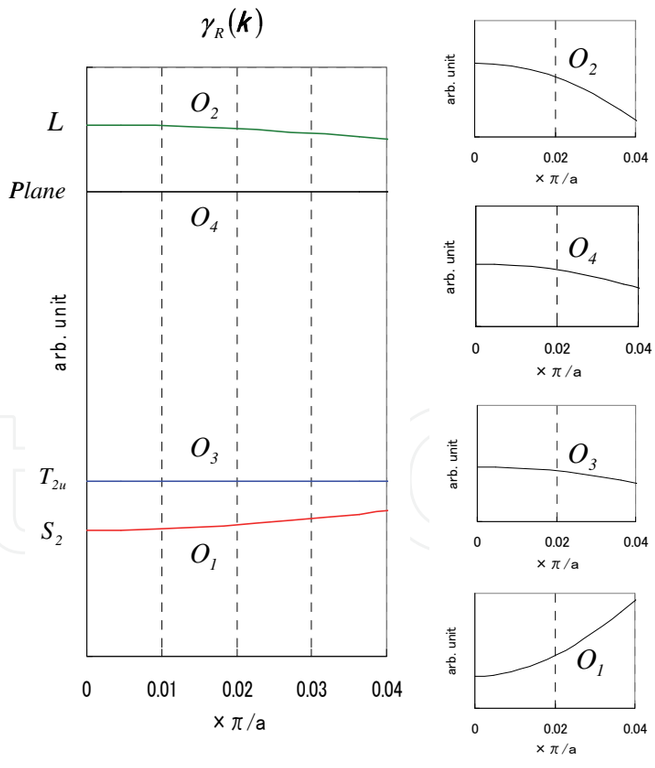

(a) (b)

Fig. 5. The function $\gamma_R(\boldsymbol{k})$ for the optical branches near Γ point. (a) The $\boldsymbol{k}$-dependence of $\gamma_R(\boldsymbol{k})$ for the optical branches derived from eq. (43) shows the softening of O_1 branch at Γ point. (b) The details obtained by magnifying the figure (a).

When the S_2 mode freezes, the $BaTiO_3$ crystal undergoes the structural phase transition from cubic to tetragonal symmetry and brings about the ferroelectricity. As a result, the author has been able to show that eq.(40) can provide the justifiable equations to determine the soft mode.

Appendix

The $BaTiO_3$ crystal with the perovskite-type structure has a property that the alloy of Ba-Ti bonding takes in the octahedron of O-O bonding by Ti-O bonding and Ba-O bonding, since the crystal is composed of three components, Ba-cubic lattice, Ti-cubic lattice and O-octahedron. As far as the author take notice of the soft mode at Γ point for the phase transition of $BaTiO_3$ at high temperature region, it is sufficient to discuss within the atomic displacements of one direction.
The equations of motion for atoms in a unit cell can be solved by applying the running wave solutions. The dynamical matrix is obtained as

$$
\boldsymbol{D} = \begin{pmatrix}
\frac{8\beta+8\gamma}{M_B} & -\frac{8\gamma\cos\frac{a}{2}k_x\cos\frac{a}{2}k_y\cos\frac{a}{2}k_z}{\sqrt{M_BM_T}} & -\frac{4\beta\cos\frac{a}{2}k_y\cos\frac{a}{2}k_z}{\sqrt{M_BM_O}} & -\frac{4\beta\cos\frac{a}{2}k_x\cos\frac{a}{2}k_z}{\sqrt{M_BM_O}} & 0 \\
-\frac{8\gamma\cos\frac{a}{2}k_x\cos\frac{a}{2}k_y\cos\frac{a}{2}k_z}{\sqrt{M_BM_T}} & \frac{2\alpha+8\gamma}{M_T} & 0 & 0 & -\frac{2\alpha\cos\frac{a}{2}k_z}{\sqrt{M_TM_O}} \\
-\frac{4\beta\cos\frac{a}{2}k_y\cos\frac{a}{2}k_z}{\sqrt{M_BM_O}} & 0 & \frac{4\beta+4\eta}{M_O} & 0 & -\frac{4\eta\cos\frac{a}{2}k_x\cos\frac{a}{2}k_z}{M_O} \\
-\frac{4\beta\cos\frac{a}{2}k_x\cos\frac{a}{2}k_z}{\sqrt{M_BM_O}} & 0 & 0 & \frac{4\beta+4\eta}{M_O} & -\frac{4\eta\cos\frac{a}{2}k_y\cos\frac{a}{2}k_z}{M_O} \\
0 & -\frac{2\alpha\cos\frac{a}{2}k_z}{\sqrt{M_TM_O}} & -\frac{4\eta\cos\frac{a}{2}k_x\cos\frac{a}{2}k_z}{M_O} & -\frac{4\eta\cos\frac{a}{2}k_y\cos\frac{a}{2}k_z}{M_O} & \frac{2\alpha+8\eta}{M_O}
\end{pmatrix} \quad \text{A - 1}
$$

where the masses of atoms are defined in Fig.1, and the force constants are represented in Fig. 2.

4. Dielectric property

It becomes to shown the relationship between the behavior of the dielectric property at high temperature region and the essential parameter at absolute zero temperature derived from the first principles calculations.

4.1 Interatomic potential

Considering that the ferroelectricity of $BaTiO_3$ mainly depends on the potential between Ti and O atoms, the author introduced the crystal potential at the nth Ti atom along the x-axis as follows (Y. Aikawa, et al., 2009):

$$
\begin{aligned}
V_n = 2D\big[&\exp(-2\alpha\Delta r)\cosh 2\alpha(x_n - < x_n >) \\
&- 2\exp(-\alpha\Delta r)\cosh\alpha(x_n - < x_n >)\big] \\
&+ C_F(x_n - < x_n >) \quad ,
\end{aligned} \tag{44}
$$

where x_n is the coordinate of the nth atom and $\langle x_n \rangle$ is the averaged equilibrium position of the n-site Ti atom along the x –axis, as shown in Fig.1, Δr is the distance between $\langle x_n \rangle$ and the minimum position, D is potential depth, $2D\alpha^2$ is the classical spring constant in the harmonic approximation, and C_F is the coefficient of the long-range order interaction.
Replacing the interatomic distance $|\boldsymbol{a}_{nn'}|$ with the atomic position x_n is expected to result in a good approximation of the nearest interaction in the neighbourhood. Then, Eqs.(17) and (29) are rewritten as follows:

$$\partial \langle V_n \rangle / \partial x_n = 0 \quad , \tag{45}$$

$$\frac{k_B T}{f^{(2)}} = \frac{f}{6\left(\delta^2 + \frac{2Cf}{v_S}\right)} \quad , \tag{46}$$

where,

$$f^{(2)} \equiv \sum_{nn'} c_S^{(nn')2} \frac{\partial^2 \langle V_n \rangle}{\partial x_n^2} \quad .$$

$$f \equiv \frac{\sum_{nn'} c_S^{(nn')2} \frac{\partial^2 \langle V_n \rangle}{\partial x_n^2}}{\sum_{nn'} c_S^{(nn')4} \frac{\partial^4 \langle V_n \rangle}{\partial x_n^4} \sum_S 1} \quad .$$

The thermal average of V_n is calculated as

$$\begin{aligned} \langle V_n \rangle = {} & 2D\exp(a_{nn'})\left[\exp(-2\alpha b_{nn'})\cosh 2\alpha\left(x - \langle x_n \rangle\right) - 2\exp(-\alpha b_{nn'})\cosh\alpha\left(x - \langle x_n \rangle\right)\right] \\ & - C_F\left(x - \langle x_n \rangle - \sum_S c_S^{(n)} \langle Q_S \rangle\right) \quad , \end{aligned} \tag{47}$$

$$a^{(nn')} \equiv -\alpha^2 \sum_S c_S^{(nn')2} \left\langle Q_S^2 \right\rangle_C - \frac{7}{12}\alpha^4 \sum_S c_S^{(nn')4} \left\langle Q_S^4 \right\rangle_C \sum_S 1$$

$$b^{(nn')} \equiv \Delta r - \frac{3}{2}\alpha \sum_S c_S^{(nn')2} \left\langle Q_S^2 \right\rangle_C - \frac{5}{8}\alpha^3 \sum_S c_S^{(nn')4} \left\langle Q_S^4 \right\rangle_C \sum_S 1$$

thus the condition of eq. (45) is

$$y^4 - e^{\alpha b_{nn'}} y^3 + \frac{C_F}{2D\alpha\exp(a_{nn'} - 2\alpha b_{nn'})} y^2 + e^{\alpha b_{nn'}} y - 1 = 0 \quad , \tag{48}$$

here

$$y \equiv \exp(\alpha x) \quad .$$

By using the solution of eq. (48), the equilibrium condition eq.(46) is as follows:

$$\frac{k_B T}{D} = \frac{2\zeta\, g(y)}{3\left(\delta^2 + \frac{2Cf(y)}{\lambda_S \gamma}\right)} \exp(a_{nn'}) \tag{49}$$

Here

$$\lambda_S \equiv \frac{\alpha^2 \mathrm{k_B} T}{2B_S}$$

$$\zeta \equiv \frac{\left(\sum_S c_S^{(nn')2}\right)^2}{\sum_S c_S^{(nn')4} \sum_S 1} \quad ,$$

$$\gamma \equiv \frac{\sum_S c_S^{(nn')4} \sum_S 1}{\sum_S c_S^{(nn')2}} \quad ,$$

$$f(y) \equiv \frac{e^{-\alpha b_{nn'}} \left(y^2 + y^{-2}\right) - \frac{1}{2}\left(y + y^{-1}\right)}{4e^{-\alpha b_{nn'}} \left(y^2 + y^{-2}\right) - \frac{1}{2}\left(y + y^{-1}\right)} \quad ,$$

$$g(y) \equiv \frac{\left[e^{-\alpha b_{nn'}} \left(y^2 + y^{-2}\right) - \frac{1}{2}\left(y + y^{-1}\right)\right]^2}{4e^{-\alpha b_{nn'}} \left(y^2 + y^{-2}\right) - \frac{1}{2}\left(y + y^{-1}\right)} e^{-\alpha b_{nn'}} \quad ,$$

The potential parameters D, α, Δr, and C_F listed in Table1 were determined with reference to the results of the first-principles calculations within the density functionl theory.

	Ferro	*Para*
C_F	1.2	0
$D[eV]$	0.094	0.2255
$\alpha[A^{-1}]$	25	25
$\Delta r[A]$	0.02833	0.02833
$C(in\ Eq.42)$	4.8×10^5	4.8×10^5

Table 1. (Y. Aikawa et al., 2009, Ferroelectrics 378)

Ultrasoft pseudopotentials (D. Vanderbilt, 1990) were used to reduce the size of the plane-wave basis. Exchange-correlation energy was treated with a generalized gradient approximation (GGA-PBE96). Y. Iwazaki evaluated the total energy differences for a number of different positions of Ti atoms positions along the *x*-axis (Fig.6) with all other atoms fixed at the original equilibrium positions, which are denoted by open circles in Fig.7. The solid lines in these figures indicate the theoretical values obtained using Eq.(44) with the fitting parameters listed in Table1.

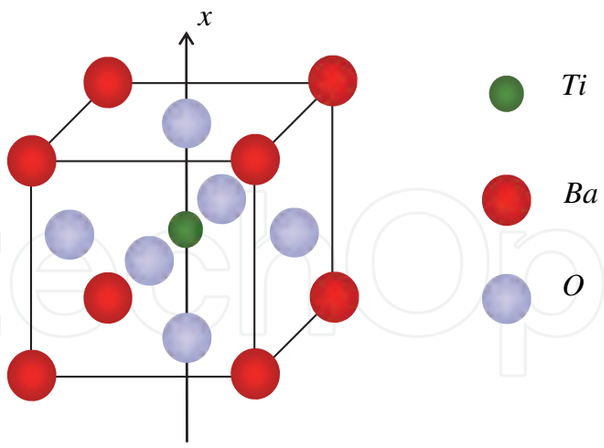

Fig. 6. Perovskite crystal structure of $BaTiO_3$

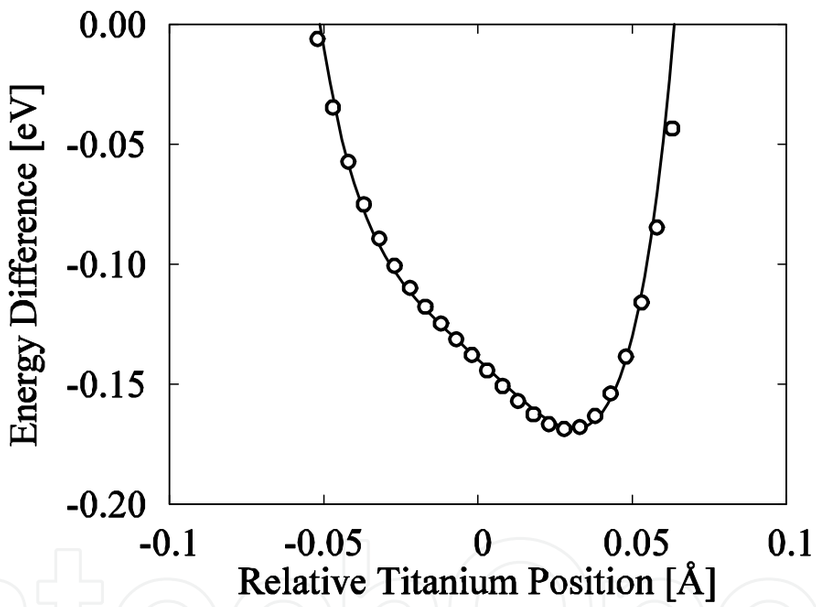

Fig. 7. Atomic potential of Ti in ferroelectric phase of $BaTiO_3$ denoted by open circles were obtained by first principles calculations, the solid line indicate theoretical values given by eq.(44) (Y. Aikawa et al., 2009, Ferroelectrics 378)

4.2 Ferroelectricity of barium titanate

When the softening occurs close to the Curie point, the solution λ_S increases rapidly. This increase implies that the second-order variational parameter B_S tends to zero, the square of the angular frequency Ω_S^2 also tends to zero because the variational parameter $2B_S$ corresponds to $M\Omega_S^2$. Thus,

$$\lambda_S \propto \frac{T}{\Omega_S^2} \quad . \tag{50}$$

The instability of the ferroelectrics in terms of the oscillator model can be explained as follows: as the temperature approaches the Curie temperature Tc, Ω_S^2 changes to zero from a positive value according to displacive ferroelectrics (B>0); Ω_S^2 changes to zero from a negative value according to the order-disorder model (B<0). The former is termed the propagation soft mode, and the latter, the non-propagation soft mode.
The relation between the dielectric constant and the frequency of an optical mode as expressed by Lyddane, Sachs and Teller (R.H.Lyddane et al.,1941) is

$$\varepsilon \propto \frac{1}{\Omega_t^2} \quad , \tag{51}$$

where Ω_t denotes the frequency of transverse optic modes. From eqs. (50) and (51), the relation between ε and λ_S is given by:

$$\frac{\varepsilon}{\varepsilon_0} = \frac{C}{T}\lambda_S \quad , \tag{52}$$

where C is a constant. The temperature dependence of λ_S is calculated by Eq.(49). Fig.8 shows the dielectric constant along the c axis measured as a function of temperature for a single crystal (W. J. Merz, 1953). The solid line in Fig.8 is fitted according to the theoretical calculation performed using Eq.(52) and the potential parameters listed in Table1.

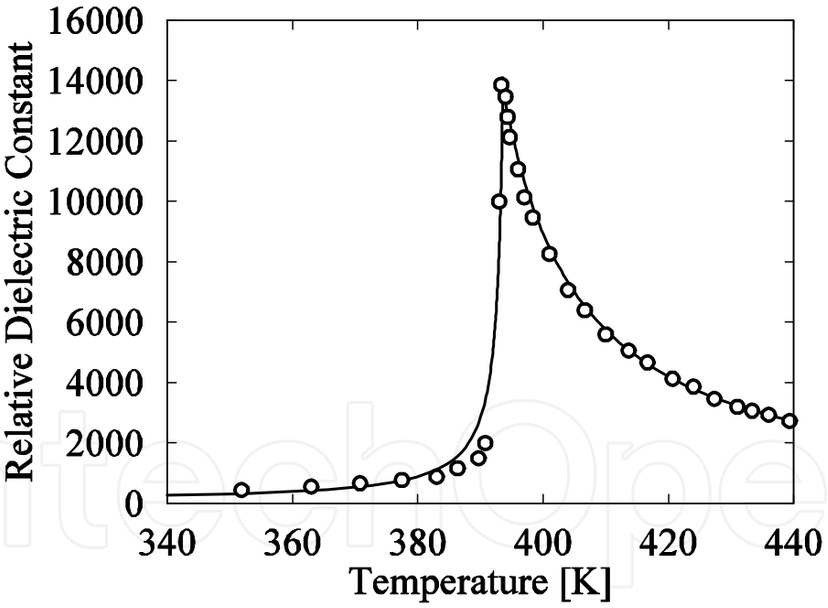

Fig. 8. Temperature dependence of the dielectric constant of single crystal of $BaTiO_3$ along the c axis. The solid line is calculated by Eq. (52), and the open circles are experimental values. (Y. Aikawa et al., 2009, Ferroelectrics 378)

5. Isotope effect

There have been some reports of the isotope effects on displacive-type phase transition, as determined experimentally (T. Hidaka & K. Oka, 1987). In classical approximation (A. D. B. Woods et al., 1960; W. Cochran, 1960), T_C is expected to shift to a higher temperature in

heavy-isotope-rich materials and vice versa. However, the experimental results are completely opposite to the expected results. It has been long considered that the origin of these phenomena in $BaTiO_3$ may be related to the quantum mechanical electron-phonon interaction (T. Hidaka, 1978, 1979).
However, it seems to be problematic to introduce the quantum mechanical electron-phonon interaction to interpret the ferroelectric phase transition in $BaTiO_3$, because the phase transition is a phenomenon in the high-temperature region in which there is scarcely any quantum effect. In order to discuss such a phenomenon in the high-temperature region, K. Fujii et al. have proposed a self-consistent anharmonic model that is applied to the phase transition (K. Fujii et al., 2001), and the author has extended it to derive the ferroelectric properties of $BaTiO_3$ (Y. Aikawa et al., 2009). In this section the isotope effect of T_C is explained through this theory, and the theoretical result is compared with experimental data.

5.1 Theory

Postulating that atomic potential is independent of atomic mass, eq. (33) is rewritten as

$$T_C = \frac{\mathrm{k_B}}{6\delta^2} \frac{\left(\left. \frac{\partial^2 \langle V \rangle}{\partial |\boldsymbol{a}_{nn'}|^2} \right|_{v_S \to \infty} \right)^2}{\left. \frac{\partial^4 \langle V \rangle}{\partial |\boldsymbol{a}_{nn'}|^4} \right|_{v_S \to \infty}} \zeta \quad , \tag{53}$$

where ζ is the mass-dependent part in T_C as

$$\zeta \equiv \frac{\left(\sum_{nn'} c_S^{(nn')2} \right)^2}{\sum_{nn'} c_S^{(nn')4} \sum_S 1} \quad . \tag{54}$$

In order to calculate eq. (54), it is necessary to obtain the eigen function $e_S^{(n)}$ in eq.(5) by solving the dynamical matrix, which consisted of atomic mass and force constants, as shown in Fig.2. The force constants shown in Fig.2 are derived from the second-order derivative of interatomic potential with respect to interatomic distance.
It is, however, difficult to estimate the force constants because estimate various interactions between atoms exist. The author did attempt to estimate them so as not to contradict the results of neutron diffraction experiments; as $(\alpha/\gamma,\ \beta/\gamma,\ \eta/\gamma)$ = (0.1, 0.09, 0.81) as derived in 3.2.

5.2 Numerical calculation and comparison with experiments

It was also shown that the soft mode is the Slater mode, which is the lowest frequency optic mode at $\boldsymbol{k}$ = 0 under this condition. Using this force constants, the ratio of T_C ($_y$Ba $_x$Ti O_3 that is replaced with isotope elements) to T_C (natural $^{137.33}$Ba $^{47.88}$Ti $^{16}O_3$) is obtained by calculating eq.(54) using x = 46-50, y =134-138 as parameters. The results are shown in Fig. 9.

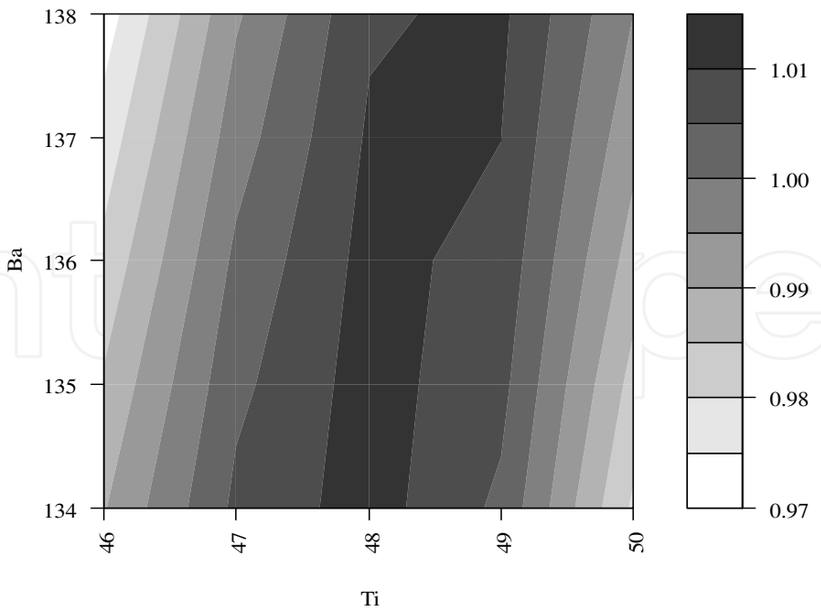

Fig. 9. x-y phase diagrams of the ratio of Tc ($_{y}Ba\ _{x}Ti\ O_3$) to Tc ($^{137.33}Ba\ ^{47.88}Ti\ ^{16}O_3$) (Y.Aikawa et al., 2010 Jpn. J. Appl. Phys. 49 09ME11)

In Fig.10, the solid curve shows the theoretical values of the transition temperature for the isotope effects of Ti calculated using eq. (54), and the experimental values are represented by open circles. It appears that the theoretical values in the solid curved line are roughly in agreement with the experimental values represented by the open circles as shown in the figure.

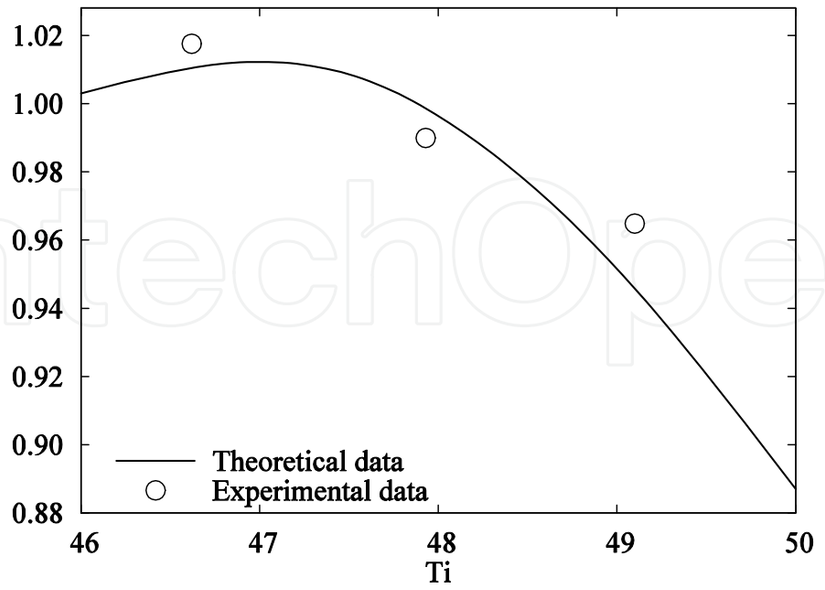

Fig. 10. Comparison between the theoretical and experimental values in terms of x-dependence of the ratio of Tc ($^{137.33}\ Ba\ _{x}Ti\ ^{16}O_3$) to Tc ($^{137.33}Ba\ ^{47.88}Ti\ ^{16}O_3$). (Y.Aikawa et al., 2010 Jpn. J. Appl. Phys. 49 09ME11)

In the case of harmonic approximation, as the heavy Ti isotope is introduced, the Curie temperature rises, and vice versa for the light Ti isotope (T. Hidaka & K. Oka, 1987), because only the coefficient $c_S^{(nn')2}$ of the harmonic term $\langle Q_S^2 \rangle$ is considered. It is known that anharmonicity promotes the instability in the crystal (K.Fujii et al., 2001), as a result, the instability undergoes the structural phase transition in the crystal systems with a strong anharmonicity. In eq.(54) the effect of the coefficient $c_S^{(nn')4}$ of the fourth-order term $\langle Q_S^4 \rangle$ is to sift T_C to the lower-temperature region, whereas that of the coefficient $c_S^{(nn')2}$ of the quadratic term $\langle Q_S^2 \rangle$ is to shift T_C to the higher-temperature region. In the higher-temperature region, the effect of $\langle Q_S^4 \rangle$ is more important. Therefore, the self-consistent anharmonic theory in the high-temperature region enables the explanation of the tendency that T_C is expect to shift to the lower temperature in the heavier Ti isotope.

The instability temperature or the transition temperature for the trial potential represented by an anharmonic oscillator has been derived from the variational method at finite temperature where the normal coordinates were introduced in this work to reflect the crystal symmetry in the softening phenomenon. The result obtained here has been applied to the isotope effect of the ferroelectric crystal $BaTiO_3$. The transition temperature T_C given by eq. (53) has been applied after substituting the actual values obtained for the force constants into ζ given by eq.(54). As a result, the author has been able to probe that the transition temperature T_C of barium titanate consisting of heavy-isotope Ti is lower than that of barium titanate consisting of light-isotope Ti.

6. Conclusion

The instability temperature or the transition temperature for the trial potential represented by an anharmonic oscillator has been derived from the variational method at finite temperature where the normal coordinates were introduced in this work to reflect the crystal symmetry in the softening phenomenon.

1. Though the expression obtained here has the same form as the Landau expansion, the transition temperature and the expansion coefficients can be represented by the characteristic constants of the potentials between atoms. From the fact that the coefficient of the second order term in the trial potential is expressed by the form such as $B_R(\boldsymbol{k})(T_C - T)$, the author has proposed the equations to determine the soft mode by imposing the condition that its $\boldsymbol{k}$ -dependent part takes the minimum value. The result obtained here has been applied to the structural phase transition of the ferroelectric crystal $BaTiO_3$. The dispersion relations derived from the dynamical matrix has been compared with that from the neutron diffraction experiment. The force constants between atoms have been fitted so as to reproduce the experimental results for the dispersion relations. The determination equations given by eq.(40) has been applied after substituted the actual values obtained for the force constants into $\gamma_R(\mathbf{k})$ given by eq.(38). As a result, the author has been able to probe that the lowest frequency mode at Γ point corresponded to the S_2 mode causing the structural phase transition in the $BaTiO_3$ crystal.
2. The author has shown that the ferroelectric properties of $BaTiO_3$ result from the equilibrium condition of free energy by using the anharmonic oscillation model and the elemental parameters derived using first-principles calculations.

3. The result obtained here has been applied to the isotope effect of the ferroelectric crystal $BaTiO_3$. The transition temperature T_C given by eq. (53) has been applied after substituting the actual values obtained for the force constants into ζ given by eq. (54). As a result, the author has been able to probe that the transition temperature T_C of barium titanate consisting of heavy-isotope Ti is lower than that of barium titanate consisting of light-isotope Ti.

7. References

Aikawa, Y. & Fujii, K. (1993). Theory of Instability Phenomena in Crystals, *J. Phys. Soc. Jpn.* 62, pp.163-169

Aikawa, Y. & Fujii, K. (1998). Theory of instability phenomena and order-disorder transition in CsCl type crystal, *Phys. Rev. B* 57, pp. 2767-2770

Aikawa, Y.; Sakashita, T.; Suzuki, T. & Chazono, H. (2007). Theoretical consideration of size effect for barium titanate, *Ferroelectrics,* 348, pp. 1-7

Aikawa, Y. & Fujii, K. (2009). Theory of instability phenomena and its application to melting in cubic metals, *Mater. Trans.* 50, pp. 249-253

Aikawa, Y.; Iwazaki, Y.; Sakashita,T. & Suzuki, T. (2009). Self-consistent anharmonic theory and its application to ferroelectric crystal, *Ferroelectrics,* 378, pp.8-15

Aikawa, Y.; Sakashita, T. & Suzuki, T. (2010). Self-consistent anharmonic theory and its application to the isotope effect on ferroelectric phase transition in $BaTiO_3$ crystal, *Jpn. J. Appl. Phys.* 49, pp. 09ME11-1～09ME11-5

Aikawa, Y.; Iwazaki, Y. & Suzuki, T. (2010). Theoretical analysis of surface effect of crystal and its application to $BaTiO_3$ fine particle, *J. Ceram. Soc. Jpn* 118, pp. 1057-1061

Akdogan, E. K. & Safari, A. (2002). Phenomenological theory of size effects on the cubic-tetragonal phase transition in $BaTiO_3$ nanocrystals, *Jpn. J. Appl. Phys.* 41, pp.7170-7175

Arlt, G.; Hennings, D. & de With, G. (1985). Dielectric properties of fine-grained barium titanate ceramics, *J. Appl. Phys.* 58, pp.1619-1625

Burns, G. (1977). Introduction to group theory with applications, *Academic Press* pp.91-93 Cochran, W. (1959). Crystal stability and the theory of ferroelectricity, *Phys.Rev.Lett.*3, pp.412-414

Cochran, W. (1960). Crystal stability and the theory of ferroelectricity *Adv. Phys.* 9, pp.387 -423

Fujii, K.; Aikawa,Y. & Ohoka, K. (2001). Structural phase transition and anharmonic effects in crystal, *Phy. Rev. B*63, pp.104107-1～104107-4

Fujii, K. ; Aikawa,Y. & Shimazutsu,Y.(2003). Instability of the order-disorder ferroelectrics, J. Phys. Soc. Jpn. 72, pp.727-729

Gillis, N. S.; Werthamer, N. R. & Koehler, T. R. (1968). Properties of crystalline argon and neon in the self-consistent phonon approximation, *Phys. Rev.*165 pp.951-959

Gills, N. S.; & Koehler, T. R. (1971). Self-consistent treatment of the frequency spectrum of a model paraelectric, *Phys. Rev. B*4, pp.3971-3982

Harada, J. & Honjo, G. (1967). X-ray studies of the lattice vibration in tetragonal barium titanate, *J. Phys. Soc. Jpn* 22, pp.45-57

Hidaka,T. (1978). Theory of a structural phase transition of $SrTiO_3$ at 110K, *Phys. Rev. B* 17, pp. 4363-4367

Hidaka, T. (1979). Electronic instability of the Γ_{15} phonon in $BaTiO_3$, *Phys. Rev. B* 20, pp.2769-2773

Hidaka, T. & Oka, K. (1987). Isotope effect on BaTiO3 ferroelectric phase transitions, *Phys. Rev. B* 35, pp.8502-8508

Hoshina,T.; Takizawa, K.; Li, J.; Kasama,T.; Kakemoto, H. & Tsurumi,T. (2008). Domain size effect on dielectric properties of barium titanate ceramics, *Jpn. J. Appl. Phys.* 47, pp.7607-7611

Hoshina,T.; Wada, S.; Kuroiwa, Y. & Tsurumi, T. (2008). Composite structure and size effect of barium titanate nanoparticles, *Appl. Phys. Lett.* 93, pp.192914-1～192914-3

Jannot, B.; Escribe-Filippini C. & Bouillot, J. (1984). Lattice dynamics of pure barium titanate and barium strontium titanate solid solutions, *J. Phys. C, Solid State Phys.*17, pp.1329-1338

Junquera, J. & Ghosez,P. (2003). Critical thickness for ferroelectricity in perovskite ultrathin films, *Nature* 422, pp.506-509.

Kishi, H.; Mizuno Y. & Chazono,H. (2003). Base metal electrode multilayer ceramic capacitors: past, present and future perspectives, *Jpn. J. Appl. Phys.* 42, pp.1-15

Landau, L. D. & Lifshitz, E. M. (1958). Statistical Physics, *Pergamon,* London Lyddane, R. H.; Sachs, R. G. & Teller, E. (1941). On the polar vibrations of Alkali halides, *Phys. Rev.*59, pp.673-676

Matsubara, T. & Kamiya, K. (1977). Self-consistent Einstein model and Theory of anharmonic surface vibration. I , *Prog. Theor. Phys.* 58, pp.767-776 Merz, W. J. (1953). Double hysteresis loop of $BaTiO_3$ at the Curie point, *Phys. Rev.* 91, pp.513-517

Ohno,T.; Suzuki, D.; Suzuki, H. & Ida, T. (2004). Size Effect for Barium Titanate Nano-particles, *KONA* 22, pp.195-201

Onodera, Y. (1970). Dynamic Susceptibility of Classical Anharmonic Oscillator, *Prog. Theor. Phys.* 44, pp.1477-1499

Perebeinos,V.; Chan, S. W. & Zhang, F. (2002). 'Madelung model' prediction for dependence of lattice parameter on nano crystal size, *Sol. State. Comm.* 123, pp.295-297

Shih, W. Y.; Shih, W. H. & Askey, I. A. (1994). Size dependence of the ferroelectric transition of small $BaTiO_3$ particles: Effect of depolarization, *Phys. Rev. B* 50, pp.15575-15585 Shirane, G.; Frazer, B. C.; Minkiewicz,V. J. & Leake, J. A. (1967). Soft optic modes in barium titanate, *Phys.Rev.Lett.*19, pp.234-235

Vanderbilt,D. (1990). Soft self consistent pseudopotentials in a generalized eigenvalue formalism, *Phys. Rev. B* 41, pp.7892-7895

Woods, A. D. B.; Cocran,W. & Brockhouse, B. N.(1960).Lattice dynamics of alkali halide crystals,*Phys. Rev.* 119, pp.980-999

Wada, S.; Yasuno, H.; Hoshina,T.; Nam, S. M.; Kakemoto, H. & Tsurumi,T. (2003). Preparation of nm-sized barium titanate fine particles and their powder dielectric properties, *Jpn. J. Appl. Phys.* 42, pp. 6188-6195

Zhong, W. L.; Wang,Y. G.; Zhang, P. L. & Qu, B. D. (1994). Phenomenological study of the size effect on phase transition in ferroelectric particles, *Phys. Rev. B*50, pp. 698-703 Zhong, W.; Vanderbilt, D. & Rabe, K. M. (1995). First principles theory of ferroelectric phase transitions for perovskites: the case of $BaTiO_3$, *Phys. Rev. B*52, pp. 6301-6312

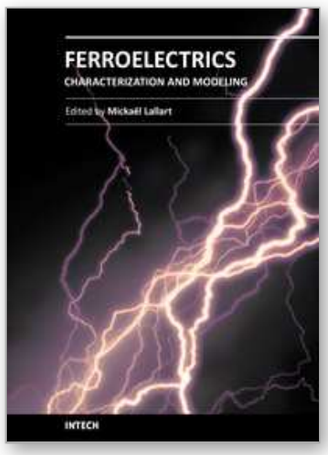

Ferroelectrics - Characterization and Modeling

Edited by Dr. MickaÃ«l Lallart

ISBN 978-953-307-455-9
Hard cover, 586 pages
Publisher InTech
Published online 23, August, 2011
Published in print edition August, 2011

Ferroelectric materials have been and still are widely used in many applications, that have moved from sonar towards breakthrough technologies such as memories or optical devices. This book is a part of a four volume collection (covering material aspects, physical effects, characterization and modeling, and applications) and focuses on the characterization of ferroelectric materials, including structural, electrical and multiphysic aspects, as well as innovative techniques for modeling and predicting the performance of these devices using phenomenological approaches and nonlinear methods. Hence, the aim of this book is to provide an up-to-date review of recent scientific findings and recent advances in the field of ferroelectric system characterization and modeling, allowing a deep understanding of ferroelectricity.

INTECH
open science | open minds

InTech Europe
University Campus STeP Ri
Slavka Krautzeka 83/A
51000 Rijeka, Croatia
Phone: +385 (51) 770 447
Fax: +385 (51) 686 166
www.intechopen.com

InTech China
Unit 405, Office Block, Hotel Equatorial Shanghai
No.65, Yan An Road (West), Shanghai, 200040, China
中国上海市延安西路65号上海国际贵都大饭店办公楼405单元
Phone: +86-21-62489820
Fax: +86-21-62489821

IntechOpen